Molecular Biology of the Cell
Vol. 13, 2031–2044, June 2002

Extracellular Signal-regulated Kinase Phosphorylates Tumor Necrosis Factor α-converting Enzyme at Threonine 735: A Potential Role in Regulated Shedding

Elena Díaz-Rodríguez, Juan Carlos Montero, Azucena Esparís-Ogando, Laura Yuste, and Atanasio Pandiella*

Instituto de Microbiología Bioquímica and Centro de Investigación del Cáncer, Consejo Superior de Investigaciones Científicas-Universidad de Salamanca, 37007-Salamanca, Spain

Submitted November 29, 2001; Revised March 8, 2002; Accepted March 20, 2002
Monitoring Editor: Marc Mumby

The ectodomain of certain transmembrane proteins can be released by the action of cell surface proteases, termed secretases. Here we have investigated how mitogen-activated protein kinases (MAPKs) control the shedding of membrane proteins. We show that extracellular signal-regulated kinase (Erk) acts as an intermediate in protein kinase C-regulated TrkA cleavage. We report that the cytosolic tail of the tumor necrosis factor α-converting enzyme (TACE) is phosphorylated by Erk at threonine 735. In addition, we show that Erk and TACE associate. This association is favored by Erk activation and by the presence of threonine 735. In contrast to the Erk route, the p38 MAPK was able to stimulate TrkA cleavage in cells devoid of TACE activity, indicating that other proteases are also involved in TrkA shedding. These results demonstrate that secretases are able to discriminate between the different stimuli that trigger membrane protein ectodomain cleavage and indicate that phosphorylation by MAPKs may regulate the proteolytic function of membrane secretases.

INTRODUCTION

The ectodomain of a number of transmembrane proteins can be released as a soluble fragment by the action of cell surface proteases, termed secretases (Ehlers and Riordan, 1991; Massagué and Pandiella, 1993; Hooper *et al.*, 1997). Proteins whose ectodomains are shed include membrane-anchored growth factors (Massagué and Pandiella, 1993), some of their receptors (Downing *et al.*, 1989; Porteu and Nathan, 1990; Prat *et al.*, 1991; Yee *et al.*, 1994; Cabrera *et al.*, 1996; Vecchi *et al.*, 1996), adhesion molecules (Kishimoto *et al.*, 1989), ectoenzymes (Sadhukhan *et al.*, 1999), and proteins such as the β-amyloid precursor protein (Selkoe, 1994; Hooper *et al.*, 1997). Alterations in the cleavage of some of these membrane proteins may lead to disease. Thus, mutations in the ectodomain of the p75 tumor necrosis factor (TNF) receptor ($p75^{TNFR}$) that decrease the shedding of its ectodomain have been linked to an autosomal dominant disease characterized by fever and severe local inflammation (McDermott *et al.*, 1999). The pathogenesis of these disease signs probably involves impaired clearance of the $p75^{TNFR}$ resulting in a decreased buffering activity of the soluble receptor, together with an increased level of the membrane holoreceptor that facilitates TNF-α responses. Another example of the importance of membrane sheddases has been obtained in animal models of pseudoinfectious or cachectic states (Gearing *et al.*, 1994; Mohler *et al.*, 1994). Injection of inhibitors of the shedding of membrane proTNF-α into rodents prevented the release of soluble TNF-α into the serum and protected these animals against a lethal dose of endotoxin (Gearing *et al.*, 1994; Mohler *et al.*, 1994).

Pharmacological experiments using inhibitors of the different protease families pointed to metalloproteases as the enzymes responsible for membrane protein ectodomain cleavage (Gearing *et al.*, 1994; McGeehan *et al.*, 1994; Mohler *et al.*, 1994). Later, by the use of these inhibitors (Moss *et al.*, 1997) and in vitro peptide cleavage assays (Black *et al.*, 1997), an enzyme, the proTNFα-converting enzyme (TACE), which

Article published online ahead of print. Mol. Biol. Cell 10.1091/mbc.01–11–0561. Article and publication date are at www.molbiolcell.org/cgi/doi/10.1091/mbc.01–11–0561.

* Corresponding author. E-mail address: atanasio@usal.es.

Abbreviations used: ADAM, a disintegrin and metalloprotease; BIM, bis-indolylmaleimide; CHO, Chinese hamster ovary; EGF, epidermal growth factor; Erk, extracellular signal-regulated kinase; GFP, green fluorescent protein; GST, glutathione *S*-transferase; HA, hemagglutinin; IRES, internal ribosomal entry site; JNK, c-Jun N-terminal kinase; MAPK, mitogen-activated protein kinase; NGF, nerve growth factor; $p75^{TNFR}$, p75 tumor necrosis factor receptor; PBS, phosphate-buffered saline; PBST, PBS supplemented with 0.1% Triton X-100, final concentration; PKC, protein kinase C; PMA, phorbol 12-myristate, 13-acetate; TACE, TNF-α–converting enzyme; TGFα, transforming growth factor α; TNF-α, tumor necrosis factor α.

participates in the solubilization of TNF-α from its precursor, was been isolated. Structurally, TACE is a type I membrane protein that contains several domains in the extracellular region, including disintegrin and metalloprotease domains, characteristic of the ADAM subfamily of metalloproteases (Blobel, 1997; Black and White, 1998). TACE may also participate in the cleavage of other transmembrane proteins, since cells from TACE-deficient animals fail to efficiently cleave protransforming growth factor α (proTGFα), L-selectin, the $p75^{TNFR}$ (Peschon *et al.*, 1998), or β-amyloid precursor protein (Buxbaum *et al.*, 1998). It is possible that other proteases may be involved in the regulation of membrane protein ectodomain cleavage. In fact, solubilization of the ectodomain of the angiotensin-converting enzyme is unaffected in fibroblasts derived from TACE-deficient animals (Sadhukhan *et al.*, 1999); studies of the solubilization of proheparin-binding epidermal growth factor (EGF)-like growth factor (proHB-EGF) have indicated that other ADAM family members, such as MDC9/ADAM9/Meltrin-γ, may also participate in the release of soluble forms of membrane-bound molecules (Izumi *et al.*, 1998).

A property of the activity of membrane secretases is its highly regulated nature. In fact, activation of intracellular second messenger systems, such as the protein kinase C (PKC) or intracellular Ca^{2+} pathways, up-regulates the activity of membrane secretases (Massagué and Pandiella, 1993). Recently, mitogen-activated protein kinase (MAPK) cascades have also been implicated in the regulation of the shedding of membrane proteins. Thus, solubilization of the membrane-anchored growth factors HB-EGF (Gechtman *et al.*, 1999) and proTGFα (Fan and Derynck, 1999), as well as the adhesion molecule L-selectin (Rizoli *et al.*, 1999), can be prevented by treatments that block MAPK activation. MAPK routes are characteristically organized into a three-kinase module that includes an MAPK, the upstream kinase MEK or MKK, which phosphorylates and activates MAPK, and the MEK kinase, which is responsible for the activation of MEK (Robinson and Cobb, 1997). Three major MAPK pathways have been described in mammals. The extracellular signal-regulated kinase (Erk) 1 and 2 route is activated by receptors for polypeptide growth factors, G protein-coupled receptors, or by directly stimulating intracellular pathways such as the PKC or calcium messenger systems (Garrington and Johnson, 1999; Widmann *et al.*, 1999). The two other MAPK routes, the p38 and the Jun N-terminal kinase (JNK) pathways, are mainly triggered by cytokine and stress stimuli (Ip and Davis, 1998; Nebreda and Porras, 2000). All MAPKs possess overlapping substrate specificities. MAPKs are proline-directed kinases that phosphorylate target proteins at serine or threonine residues with a minimum sequence of Thr/Ser-Pro. In addition, a Pro residue in the -2 position facilitates the preference of MAPKs for their substrates (Widmann *et al.*, 1999). Besides containing a potential phosphorylation site, MAPKs appear to recognize their targets by interaction with docking sites in substrates, which often include a positively charged region (Tanoue *et al.*, 2000).

During studies aimed at elucidating the mechanisms controlling the regulated cleavage of the TrkA neurotrophin receptor, we found that multiple MAPK pathways act as intermediates in PKC- and stress-induced TrkA cleavage. PKC-induced cleavage was impaired in cells derived from mice expressing an inactive form of the secretase TACE. However, stress-induced cleavage occurred in these cells, suggesting that TrkA cleavage is a complex process regu-

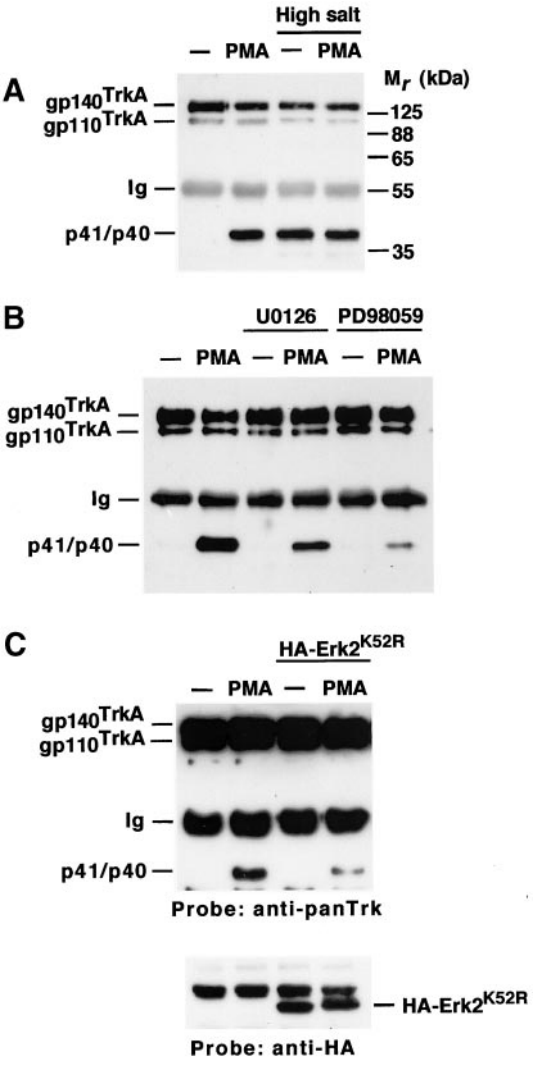

Figure 1. (A) Osmotic stress induces TrkA cleavage. CHO^{TrkA} cells were treated with PMA (1 μM) or high salt (1 M NaCl) for 30 min, followed by immunoprecipitation and Western analysis with the anti-panTrk antiserum. p41/p40 denotes TrkA fragments generated upon holoreceptor cleavage. Ig, immunoglobulin heavy chain. M_r markers are shown at the right. (B) Effect of the Erk1/2 pathway inhibitors PD98059 and U0126 on PMA-induced TrkA cleavage. CHO^{TrkA} cells were preincubated with the inhibitors (P98059: 50 μM; U0126: 10 μM) for 30 min before PMA addition. Immunoprecipitation and Western analysis was performed with the anti-panTrk antiserum. (C) Effect of a dominant negative form of Erk2 on PMA-induced TrkA cleavage. 293^{TrkA} cells were transfected with a plasmid encoding an HA-tagged dominant negative form of Erk2 ($HA\text{-}Erk2^{K52R}$). PMA treatment, immunoprecipitation, and Western analysis of TrkA cleavage was as above. Western blotting of cell lysates with the anti-HA antibody showed the mutated form of Erk2 ($HA\text{-}Erk2^{K52R}$) in the corresponding transfectants.

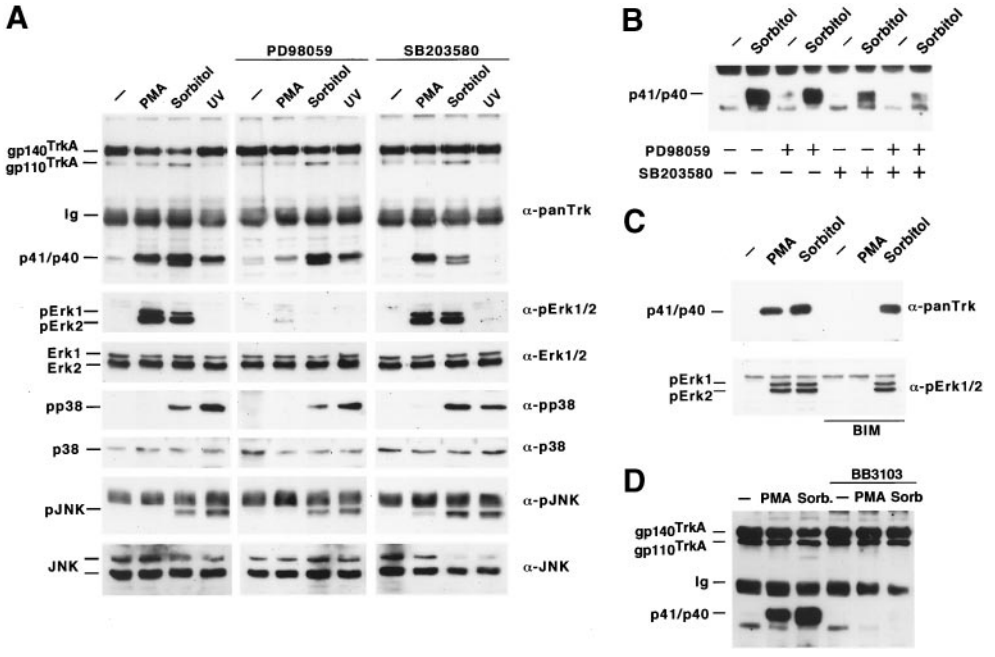

Figure 2. Multiple MAPK pathways participate in TrkA ectodomain shedding. (A) Effect of different treatments and MAPK inhibitors on TrkA cleavage. PMA or UV irradiation was used as an activator of Erk1/2 or the p38 and JNK stress pathways, respectively, whereas sorbitol was used as a nonspecific activator of MAPK pathways. Where indicated, CHO^{TrkA} cells were preincubated with PD98059 (50 μM) or SB203580 (10 μM) for 30 min before PMA, sorbitol, or UV treatment. Cell lysates were analyzed with the corresponding antibodies (indicated at the right of each panel), except for anti-panTrk and anti-pJNK, for which the samples were immunoprecipitated with anti-panTrk and anti-JNK antibodies before Western analysis. (B) Effect of PD98059 and SB203580 on TrkA cleavage. Inhibitors were added to cells, where indicated, before sorbitol treatment. TrkA cleavage was analyzed as described above. (C) Activation of Erk1/2 by sorbitol is independent of PKC. BIM (10 μM) was added to cells for 15 min before PMA or sorbitol and TrkA cleavage was analyzed as above. pErk1/2 was analyzed in cell lysates by Western blotting with an antibody that recognizes the dually phosphorylated forms of Erk1 and Erk2. (D) The metalloprotease inhibitor BB3103 prevents sorbitol and PMA-induced TrkA cleavage. BB3103 (30 μM) was added to cells for 30 min before sorbitol or PMA treatment, and TrkA cleavage was analyzed by immunoprecipitation and Western blotting as described.

lated by different proteases and signaling pathways. The MAPK Erk and TACE coprecipitated, and Erk was able to phosphorylate TACE at threonine 735. These studies identified TACE as a novel Erk substrate and indicate that MAPKs, in addition to their roles as intermediates in membrane-nuclear signaling, may also regulate inside-out signaling by directly controlling the function of membrane secretases.

MATERIALS AND METHODS

Immunochemicals, Immunoprecipitations and Western Blotting

The mAb MGR12 was obtained from Dr. S. Ménard (Istituto Nazionale dei Tumori, Milan, Italy), the M220 anti-TACE antibody was from Dr. R.A. Black (Immunex, Seattle, WA), and the mAb anti-hemagglutinin (HA) was from BABCO (Richmond, CA). Various polyclonal antisera were raised by injecting peptides corresponding to the C terminus of human TrkA, TACE, or p38 into rabbits. The anti-panTrk antiserum has been described (Cabrera *et al.*, 1996). The anti-TACE antiserum corresponded to the C terminus of human TACE (NH_2-CKLQRQNRVDSKETE-COOH). The anti-p38 antiserum was raised to the peptide NH_2-CSQERPTFYRQELN-COOH. The anti-pErk, anti-JNK, anti-pJNK, and anti-Erk2 were from Santa Cruz Biotechnology (Santa Cruz, CA). The anti-pp38 and the anti-pTP antibodies were from New England Biolabs (Beverly, MA). Immunoprecipitations and Western analyses were performed as described by Cabrera *et al.* (1996). EGF was from Collaborative Research (Bedford, MA), and NGF was from UBI (Lake Placid, NY).

Construction of Mutants, Transfections, and Production of Retrovirus

A TACE form mutated in the putative phosphorylation site that substituted threonine 735 for alanine (TACE-T^{735}A) was generated by oligonucleotide-directed mutagenesis. Extracellularly HA-tagged TACE and TACE-T^{735}A were obtained by insertion of a PCR-amplified HA-coding fragment into the naturally occurring *Eco*RI restriction site located in the ectodomain of TACE. The tagged constructs were subcloned into the pCDNA3 vector and were used to transfect 293 cells. Clones were selected with geneticin (500 μg/ml). In parallel, these forms of TACE were subcloned into the *Bam*HI-*Xho*I sites of the pLZR-internal ribosomal entry site (IRES)-green fluorescent protein (GFP) retroviral vector. A dominant negative kinase dead form of Erk2 tagged at the N terminus with an HA epitope (HA-$Erk2^{K52R}$) was provided by Dr. P. Crespo (Instituto de Investigaciones Biomédicas, Madrid, Spain). For the production of this dominant negative form in retrovirus, a 1.25-kb fragment obtained by digestion with *Hin*dIII-*Pst*I, was blunt ended and ligated to the pLZR-IRES-GFP vector after *Xho*I digestion of the vector and blunt end creation with Klenow.

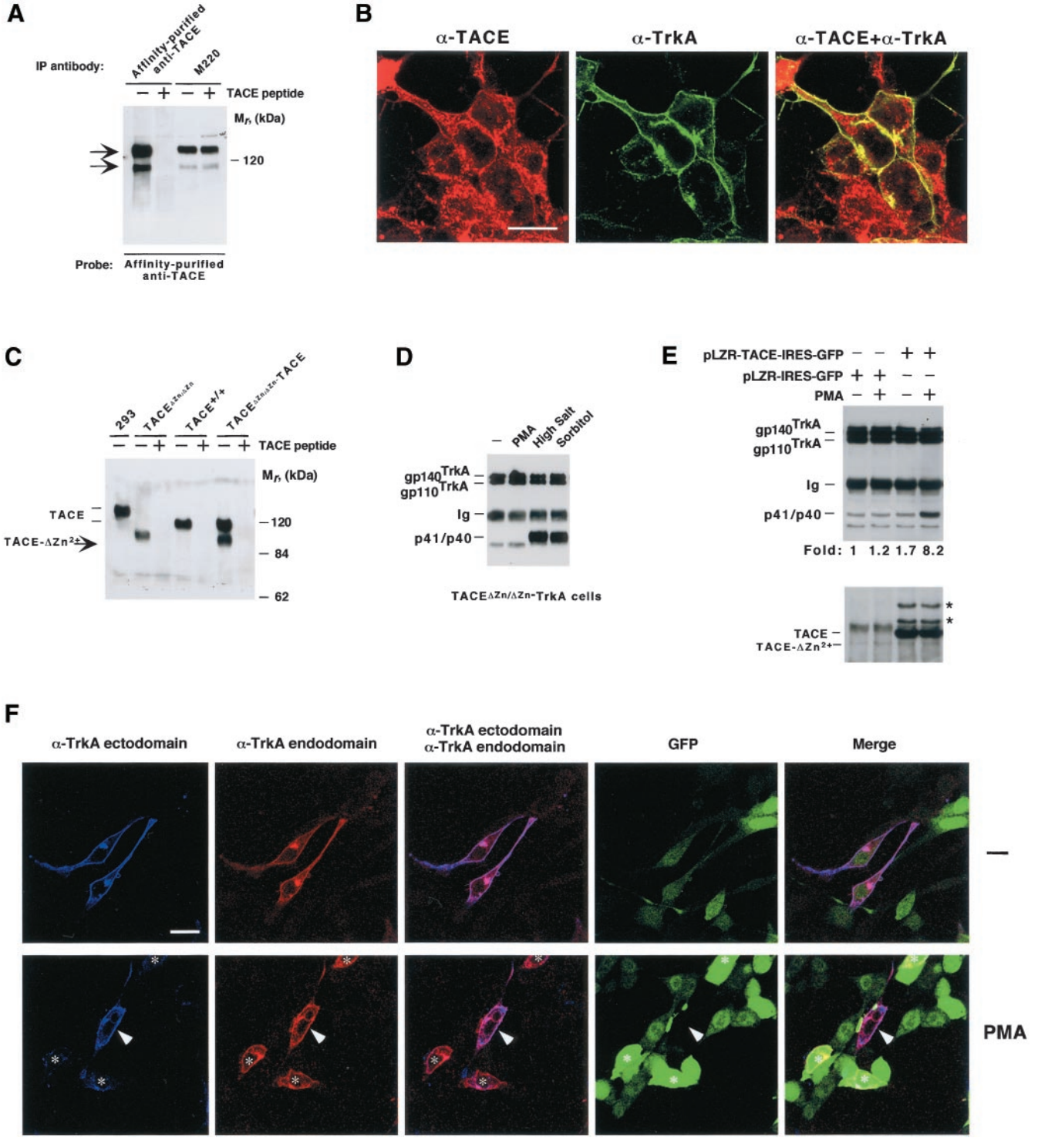

Figure 3. Participation of TACE in TrkA cleavage. (A) A polyclonal affinity-purified antibody to the C terminus of TACE or the monoclonal M220 antibody was used to immunoprecipitate TACE from lysates of 293 cells. Where indicated, 10 μg of the peptide used for the generation of the polyclonal antibody (TACE peptide) were added to the immunoprecipitates. Western analysis was performed with the affinity-purified anti-TACE antibody. (B) Distribution of TACE and TrkA in 293^{TrkA} cells. Monolayers were fixed, permeabilized, and incubated with affinity-purified anti-TACE or anti-TrkA ectodomain antibody MGR12, and images were taken in a confocal microscope. Bar, 15 μm. (C) Expression of TACE and TACE-ΔZn. Lysates from fibroblasts derived from wild-type ($TACE^{+/+}$) and $TACE^{\Delta Zn/\Delta Zn}$ animals were analyzed by immunoprecipitation and Western blotting with the affinity-purified anti-TACE antibody. Where indicated, 10 μg of the TACE peptide

TACE$^{\Delta Zn/\Delta Zn}$ fibroblasts (Peschon *et al.*, 1998) were transfected by lipofection (LipofectAMINE, Life Technologies, Carlsbad, CA) and clones and pools selected with puromycin (4 μg/ml) or infected with retrovirus. For the latter, 293T cells were plated at 1.8×10^6 cells/60-mm dish. The following day, and ~5 min before transfection, 25 μM chloroquine was added to each plate. The transfection solution was DNA (2.5 μg of pMD-G, 5 μg of pNGVL-MLV-gag-pol, 3 μg of retroviral vector), 2 M $CaCl_2$ (61 μl), and double distilled H_2O to 500 μl. Once mixed, the solution was bubbled for 15 s before its addition to the cells. Twenty-four hours later, the medium was replaced with 3 ml of fresh "virus-collecting medium," and retrovirus was recovered 1 d later. Target cells were then infected with viral supernatants containing 6 μg/ml Polybrene (Sigma, St. Louis, MO).

Glutathione S*-transferase (GST) Fusion Proteins and Fusion Protein Precipitation Experiments*

GST-Erk, GST-Elk, GST-TACE, or GST-TACE-T^{735}A, were generated according to standard protocols (Guan and Dixon, 1991). For precipitation experiments, 30 μg of the corresponding uneluted GST-fusion protein were incubated for 1 h at 4°C in 25 mM HEPES, pH 7.4; 1 mM EDTA; and 1 mM dithiothreitol, before the addition of lysates from treated cells. The lysates were then incubated for 2 h with the beads at 4°C, and then complexes were washed three times with ice-cold phosphate-buffered saline (PBS). Electrophoretic and blotting analyses were performed as described above.

In Vitro Kinase Assays

Extracts from HeLa or 293 cells treated with or without phorbol 12-myristate 13-acetate (PMA) were immunoprecipitated with the anti-Erk2 antibody, and immunocomplexes were washed three times with lysis buffer. A final wash was performed with kinase buffer (20 mM HEPES, pH 7.6; 20 mM $MgCl_2$; 25 mM β-glycerophosphate; 0.1 mM sodium orthovanadate; 2 mM dithiothreitol). The immunocomplexes were then incubated for 30 min at 30°C with the substrate in the kinase buffer containing 15 μM ATP, 1 μCi of (γ-^{32}P)ATP, and 10 μg of GST-TACE or GST-TACE-T^{735}A. To detect whether GST-Erk was able to phosphorylate GST-TACE or GST-TACE-T^{735}A, the kinase reaction was performed as described, but 10 μg of GST-Erk were included in the reaction. Samples were electrophoresed in 10% SDS-PAGE gels that were dried. Bands in gels were detected by autoradiography.

Phosphoamino Acid Analysis

The method for two-dimensional phosphoamino acid analysis has been described in detail (Cooper *et al.*, 1983). Briefly, in vitro phosphorylated GST-TACE or GST-TACE-T^{735}A was excised from dried gels and rehydrated in 50 mM ammonium bicarbonate (1.2 ml). Then, 50 μl of β-mercaptoethanol and 10 μl of 10% SDS were added, and the samples were boiled for 5 min. Proteins were eluted overnight at 37°C and precipitated with trichloroacetic acid, and pellets were washed with ethanol. Samples were dissolved in 6 M HCl, incubated for 60 min at 110°C, and dried. The hydrolysis products were separated in thin-layer chromatography plates by electrophoresis at pH 1.9 (formic acid:acetic acid:water, 50:156:1794) for 35 min at 1.5 kV, followed by a second dimension run at pH 3.5 (acetic acid:pyridine:water, 10:1:189) for 22 min at 1.3 kV, and then exposed to autoradiography.

In Vivo Phospholabeling of TACE

293 cells were incubated for 3 h in phosphate-free DMEM, and then fresh medium containing 0.5 mCi/ml [^{32}P]orthophosphoric acid was added. Cells were labeled for 3.5 h and then treated as indicated. Monolayers were washed twice in PBS and lysed in 10 mM Tris, pH 8.0; 150 mM NaCl; 1% Triton X-100; 0.1 mM sodium orthovanadate; 1 mM NaF; 1 mM phenylmethylsulfonyl fluoride; 1 μg/ml pepstatin; 10 μg/ml aprotinin; and 1 μg/ml leupeptin. Samples were then immunoprecipitated for 2 h with the anti-TACE antibody. Protein A was added for the last 20 min, and immunocomplexes were washed three times with 10 mM Tris, pH 8.0; 150 mM NaCl; and 0.1% Triton X-100, once in the same buffer supplemented with 0.5 M NaCl, and twice more in the first buffer. Samples were electrophoresed in 6% SDS-PAGE gels and dried, and bands were detected by autoradiography.

Reconstitution of TrkA Cleavage in TACE$^{\Delta Zn/\Delta Zn}$ Cells

TACE$^{\Delta Zn/\Delta Zn}$-TrkA cells were plated at a density of 10^6 cells/60-mm plate and infected with retrovirus that included the pLZR-IRES-GFP, pLZR-TACE-T^{735}A-IRES-GFP, or pLZR-TACE-IRES-GFP vectors, as described above. The cells were infected for 24 h and then replated into two 100- or 60-mm dishes. Two days later, cells were treated or not for 30 min with PMA and then lysed to be immunoprecipitated with anti-panTrk antibodies, followed by Western analyses with the same antibodies.

To visually inspect TrkA cleavage, TACE$^{\Delta Zn/\Delta Zn}$-TrkA cells were infected with the wild-type TACE retrovirus, and then cells were plated on coverslips. Cells treated or not with PMA were then washed with PBS and fixed in *p*-formaldehyde. Monolayers were washed twice in PBS supplemented with 0.1% Triton X-100 (final concentration; PBST), blocked in PBST with 5% bovine serum albumin for 1 h at room temperature, and then incubated for 2 h with the MGR12 mAb anti-TrkA ectodomain antibody, and with the anti-panTrk polyclonal affinity-purified antibody. After two washes of 15 min each in PBST, the coverslips were incubated for 30 min with a mixture of anti-mouse-Cy5 and anti-rabbit-Cy3-conjugated secondary antibodies. The coverslips were washed three times, 5 min each, in PBST and mounted. Samples were then analyzed for the presence of TrkA by immunofluorescence using an LSM510 confocal laser scanning microscope (Zeiss, Thornwood, NY). To avoid interference between fluorescence signals, the images were captured under multitracking mode.

Figure 3 (cont). were included in the immunoprecipitates. TACE immunoprecipitated from 293 cells is shown at the left. (D) Accumulation of cell-bound TrkA-truncated fragments in TACE$^{\Delta Zn/\Delta Zn}$–TrkA cells. Lysates from TACE$^{\Delta Zn/\Delta Zn}$–TrkA cells were treated with PMA (1 μM), high salt (1 M NaCl), or sorbitol (0.5 M) for 30 min, immunoprecipitated, and analyzed by Western blotting with the anti-panTrk antiserum. (E) Biochemical evidence that TACE can rescue TrkA cleavage. TACE$^{\Delta Zn/\Delta Zn}$–TrkA cells were infected with retrovirus containing pLZR-TACE-IRES-GFP or pLZR-IRES-GFP and treated with PMA where indicated. Lysates were analyzed for TrkA cleavage (top) or TACE content by Western blotting. The asterisks denote two additional bands present in cells infected with pLZR-TACE-IRES-GFP. (F) Reconstitution of TrkA ectodomain cleavage in TACE$^{\Delta Zn/\Delta Zn}$–TrkA cells. Cells were infected with the retrovirus with the pLZR-TACE-IRES-GFP vector and treated (bottom) or not (top) with PMA for 30 min. Cells were then fixed, permeabilized, and incubated with the anti-TrkA ectodomain and endodomain antibodies, followed by secondary antibodies labeled with Cy5 (blue, anti-mouse) or Cy3 (red, anti-rabbit). Triple color images were obtained in a confocal microscope. Notice that cells with a high GFP (and thus TACE, asterisks) amount had lost most of the blue (ectodomain epitope) fluorescence but still kept high amounts of red (endodomain epitope) signal in cells treated with PMA. The central cell in the bottom (arrowhead), which did not capture pLZR-TACE-IRES-GFP, did not respond to PMA by a decrease in ectodomain staining. Bar, 30 μm.

RESULTS

Multiple MAPK Pathways Regulate TrkA Cleavage

Regulated TrkA cleavage can be easily followed in Chinese hamster ovary (CHO) cells transfected with the cDNA coding for the human version of the receptor (CHO^{TrkA} cells; Cabrera *et al.*, 1996). Immunoprecipitation and Western blot analysis of CHO^{TrkA} cell lysates with an anti-panTrk antiserum raised to the cytosolic C terminus of TrkA identified two forms of the receptor: $gp110^{TrkA}$ and $gp140^{TrkA}$ (Figure 1A). In addition to these holoreceptor forms, lower M_r fragments (p41 and p40) were identified by this antiserum in cells treated with the PKC activator PMA (Figure 1A; Cabrera *et al.*, 1996; Diaz-Rodriguez *et al.*, 1999). These lower M_r forms represent truncated forms of the receptor that contain the transmembrane and cytosolic domains (Cabrera *et al.*, 1996; Diaz-Rodriguez *et al.*, 1999).

During studies to evaluate whether the TrkA-processing protease was membrane bound, we noticed that treatment of cultured cells with high salt (1 M NaCl) stimulated processing of the receptor (Figure 1A). Treatment of CHO^{TrkA} cells with sorbitol mimicked the effect of NaCl on TrkA cleavage (Figure 2; Díaz-Rodríguez, Montero, Esparís-Ogando, Yuste, and Pandiella, unpublished data), indicating that changes in medium osmolarity can stimulate cleavage independently of the effect of NaCl on membrane potential. Because changes in medium osmolarity had been reported to regulate the shedding of L-selectin through MAPK routes (Rizoli *et al.*, 1999), the above data raised the possibility that TrkA cleavage induced under these treatments could be mediated by the activation of these routes. To further explore this possibility we used PD98059 and U0126, two drugs that inhibit Erk upstream-activating kinases (Dudley *et al.*, 1995; Favata *et al.*, 1998) and have been reported to affect the shedding of other membrane-bound molecules (Fan and Derynck, 1999; Gechtman *et al.*, 1999). Preincubation with PD98059 or U0126 resulted in a significant inhibition of PMA-induced TrkA cleavage (Figure 1B). The extent of this inhibition varied from 30–90% depending on the cell line (see below; Díaz-Rodríguez, Montero, Esparís-Ogando, Yuste, and Pandiella, unpublished data). In addition, transfection of TrkA-expressing 293 cells (293^{TrkA} cells) with a dominant negative form of Erk2 partially inhibited PMA-induced TrkA cleavage (Figure 1C).

To investigate whether different MAPKs were involved in TrkA cleavage, specific inhibitors of the Erk1/2 and p38 MAPK routes were used, combined with an analysis of the activation of different MAPKs using phosphorylation state-specific antibodies. PMA treatment resulted in Erk1/2 phosphorylation (Figure 2A, second left panel). In contrast, this treatment did not significantly stimulate p38 or JNK phosphorylation (Figure 2A, fourth and sixth panels). Induction of stress by sorbitol or UV irradiation stimulated the p38 and JNK pathways (Figure 2A, fourth and sixth panels). Like PMA, sorbitol was also able to stimulate Erk1/2 phosphorylation (Figure 2A, second left panel). Erk1/2 activation by phorbol esters or sorbitol was prevented by preincubation with PD98059, indicating that both agents act on Erk upstream-activating kinases (Figure 2A, second central panel). In contrast, SB203580, an inhibitor of the p38 pathway that acts downstream of the p38 kinase (Cohen, 1997), did not prevent PMA or sorbitol-induced Erk1/2 activation (Figure 2A, second right panel). The action of sorbitol on Erk1/2 activation was not mediated by stimulation of PKC, as indicated by the failure of the PKC inhibitor bis-indolylmaleimide (BIM) to prevent Erk1/2 activation (Figure 2C). BIM was also unable to prevent sorbitol-induced TrkA processing, indicating that the action of sorbitol on TrkA cleavage was independent of PKC.

Preincubation with PD98059 significantly inhibited PMA-induced TrkA cleavage (Figure 2A, top central panel). SB203580 largely inhibited sorbitol-induced TrkA cleavage, leaving unaffected the ability of PMA to induce TrkA cleavage (Figure 2A, top right panel). Preincubation with both PD98059 and SB203580 had a more profound inhibitory effect on sorbitol-induced TrkA cleavage than treatment with each inhibitory drug alone (Figure 2B), indicating that the action of sorbitol on TrkA cleavage probably depends on the activation of both p38 and Erk1/2. UV irradiation, which activated the p38 and JNK routes, also induced TrkA cleavage (Figure 2A, top left panel). This effect was abolished by preincubation with SB203580 (Figure 2A, top right panel), indicating that UV irradiation stimulated TrkA cleavage through a p38-dependent route.

Hydroxamic acid-derived metalloprotease inhibitors can prevent the release of the ectodomain of several membrane proteins (Blobel, 1997; Black and White, 1998). To investigate whether the different MAPK routes converged in the activation of analogous protease activities, we used the metalloprotease inhibitor BB3103. As shown in Figure 2D, preincubation of cells with this inhibitor prevented the stimulated cleavage of TrkA by PMA or sorbitol. The effect of BB3103 was dose dependent with IC_{50} values (250 nM for PMA and 800 nM for sorbitol, Díaz-Rodríguez, Montero, Esparís-Ogando, Yuste, and Pandiella, unpublished data) known to specifically act on metalloproteases (Gearing *et al.*, 1994).

PKC-induced TrkA Cleavage Is Impaired in Fibroblasts Expressing an Inactive Form of TACE

The protease TACE/ADAM17 has been isolated with metalloprotease inhibitors of the hydroxamic acid family (Black *et al.*, 1997; Moss *et al.*, 1997). This secretase has been implicated in the shedding of several membrane proteins (Peschon *et al.*, 1998). To analyze whether this protease was involved in the cleavage of TrkA, we first investigated whether TrkA and TACE colocalized. For this, an antibody toward the intracellular C terminus of TACE was raised. In human 293 cells this antibody recognized two bands whose presence was prevented by preincubation with the peptide used for immunization (Figure 3A). The amount of the faster migrating form, which may represent immature or truncated TACE, was variable (Figure 3, A and C). These TACE forms were also recognized by the M220 mAb, which has previously been shown to interact with the ectodomain of human TACE (Black *et al.*, 1997; Doedens and Black, 2000). Immunofluorescence staining with the purified polyclonal antibody showed that TACE accumulated in several locations, including the plasma membrane, the perinuclear area, and other cytosolic locations where staining was characterized by a dotted pattern (Figure 3B). This staining was prevented by preincubation of the anti-TACE antibody with the TACE peptide, and no staining was observed when using another affinity-purified control antibody (Díaz-Rodríguez, Montero, Esparís-Ogando, Yuste, and Pandiella, un-

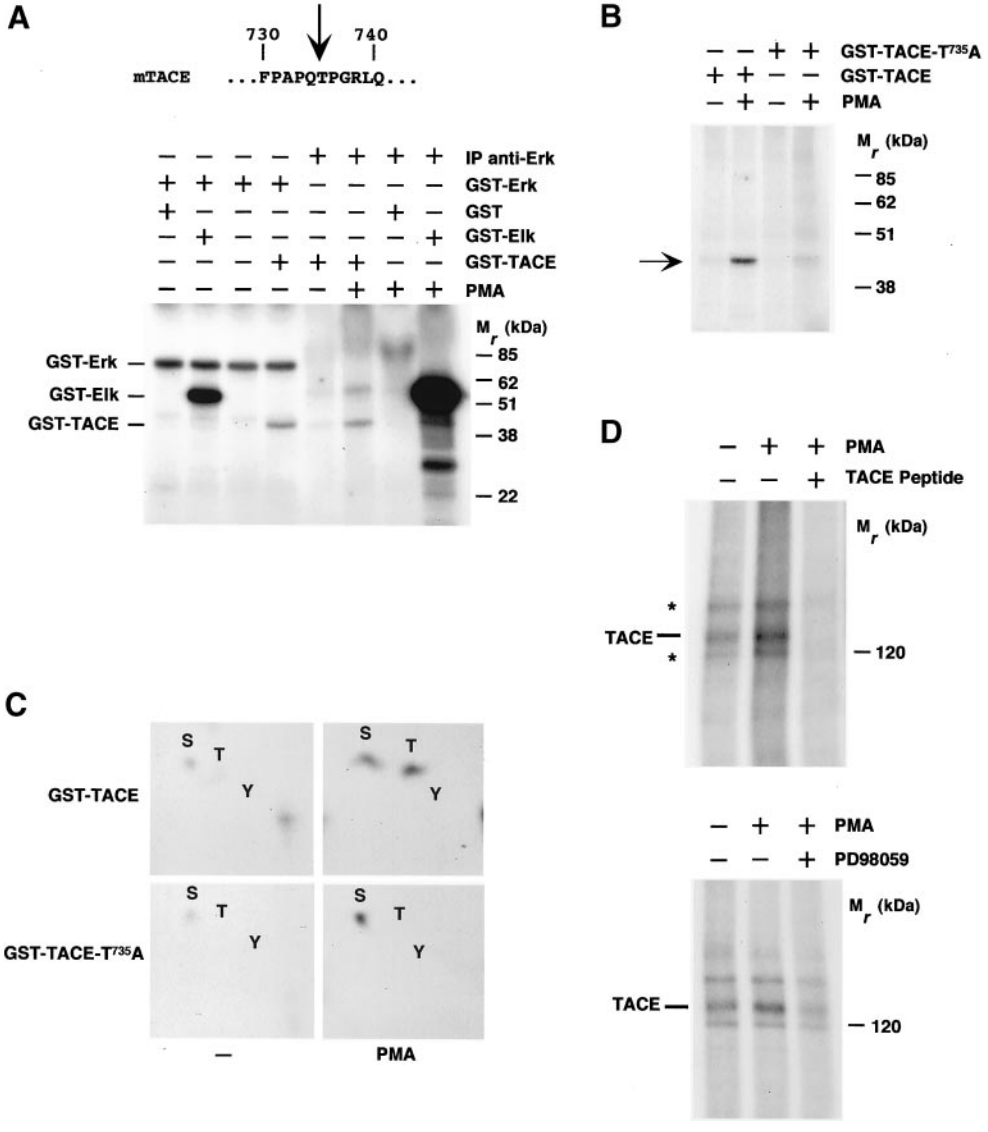

Figure 4. Phosphorylation of TACE by Erk. (A) Primary sequence of a region of the mouse TACE intracellular domain indicating (arrow) a potential MAPK phosphorylation site. Bottom, an autoradiogram of an in vitro phosphorylation of TACE by Erk. Assays were performed by using bacterially produced GST-Erk or anti-Erk immunoprecipitates (IP anti-Erk) as the enzyme and 10 μg of GST, GST-Elk or GST-TACE as the substrate. To obtain activated Erk from HeLa cell lysates, cells were treated with PMA for 30 min before lysis and immunoprecipitated with the anti-Erk antibody. (B) Results from an in vitro kinase assay using bacterially produced GST-TACE or GST-TACE-T^{735}A. Lysates from control or PMA-treated HeLa cells were immunoprecipitated with the anti-Erk antibody, and the immunoprecipitates were tested for their ability to phosphorylate in vitro 10 μg of GST-TACE or GST-TACE-T^{735}A. The amounts of the recombinant proteins used in the kinase assays were verified by Coomassie staining of gels run in parallel (Díaz-Rodríguez, Montero, Esparís-Ogando, Yuste, and Pandiella, unpublished data). (C) Phosphoamino acid analysis of an experiment identical to that shown in B. The phosphorylated bands were excised, proteins were eluted and hydrolyzed, and phosphoamino acids were identified by two-dimensional electrophoresis. (D) In vivo phosphorylation of TACE by PMA. Top, 293 cells labeled with ^{32}P were treated with PMA for 30 min where indicated. TACE was immunoprecipitated with the anti-TACE antibody, and the immunoprecipitates were analyzed by SDS-PAGE, followed by autoradiography. An additional PMA-treated sample was incubated with an excess (10 μg) of the peptide used to raise the anti-TACE antiserum. The asterisks indicate the position of two bands of unknown identity. Bottom, effect of the Erk pathway inhibitor PD98059 on TACE phosphorylation. Where indicated, cells labeled with ^{32}P were incubated with PD98059 (50 μM) for 30 min before PMA treatment. Lysates were immunoprecipitated with the anti-TACE antibody, followed by SDS-PAGE and autoradiography.

published data). TrkA staining at the cell periphery was more prominent than that of TACE, and the receptor also accumulated in an intracellular perinuclear region (Figure 3B). Merging of both immunofluorescence images indicated that TACE and TrkA colocalized at the plasma membrane and in the perinuclear area. Interestingly, TrkA staining was

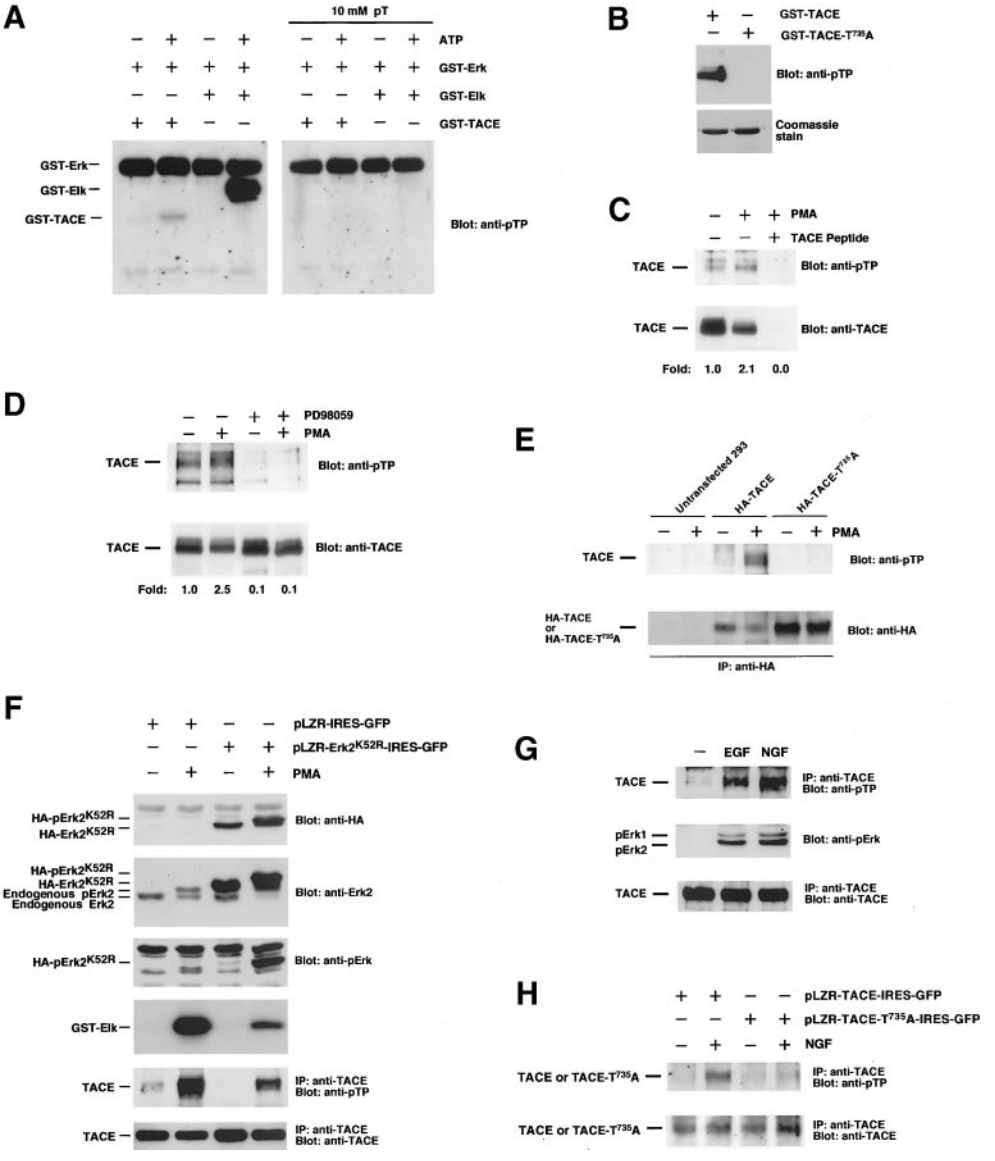

Figure 5. Erk phosphorylates TACE at T^{735} in vivo. (A) Immunoreaction of the anti-pTP antibody with phosphorylated GST-TACE and GST-Elk. GST-TACE or GST-Elk was subjected to in vitro phosphorylation using cold ATP as the phosphate donor and GST-Erk as the enzyme. Reactions were stopped by the addition of sample buffer and divided into two aliquots that were subjected to electrophoresis in 12% SDS-PAGE gels. The gel was blotted to an Immobilon membrane that was divided in two identical parts. One was probed with the anti-pTP antibody, and the other was probed with the same antibody that had previously been preadsorbed with 10 mM phosphothreonine. (B) The anti-pTP antibody failed to react with GST-TACE-T^{735}A. GST-TACE or GST-TACE-T^{735}A was subjected to in vitro phosphorylation using cold ATP as the phosphate donor and immunoprecipitated Erk as the enzyme. Reactions were stopped by the addition of sample buffer and divided into two aliquots that were subjected to electrophoresis in 12% SDS-PAGE gels. One of the gels was blotted to an Immobilon membrane that was probed with the anti-pTP antibody (top); the other gel was stained with Coomassie (bottom). (C) PMA increased phosphorylation of TACE at T^{735}. Where indicated, 293 cells were treated with PMA and okadaic acid (1 μM) for 30 min and then lysed and immunoprecipitated with the anti-TACE antibody. An additional PMA-treated sample was incubated during the immunoprecipitation with an excess (10 μg) of the peptide used to raise the anti-TACE antiserum. The immunoprecipitates were analyzed by SDS-PAGE, followed by Western blotting with the anti-pTP antibody (top). The amount of TACE present in the immunoprecipitated samples was analyzed after stripping and reprobing of the blot with the anti-TACE antibody (bottom). The signals were quantitated using the NIH Image 1.6 software, and the anti-pTP/anti-TACE ratio was calculated. A ratio of 1 was considered that of the untreated control sample. (D) Effect of PD98059 on TACE T^{735} phosphorylation. Where indicated, cells were incubated with PD98059 (50 μM) for 30 min before PMA treatment. Lysates were immunoprecipitated with the anti-TACE antibody, and Western blots were probed with anti-pTP (top) or anti-TACE antibodies (bottom). (E) In vivo phosphorylation of TACE at T^{735} detected by Western blotting with the anti-pTP antibody. 293 cells transfected with HA-TACE or HA-TACE-T^{735}A were treated with PMA, immunoprecipitated with the anti-HA antibody, and Western blots were probed with anti-pTP (top). After stripping, the blot was reprobed with anti-HA (bottom). (F) Effect of a dominant negative form of Erk2 on TACE phosphorylation

excluded from the regions of the cytoplasm where a dotted distribution of TACE was observed. Treatment of cells with PMA or sorbitol did not substantially affect the cellular distribution of TACE (Díaz-Rodríguez, Montero, Esparís-Ogando, Yuste, and Pandiella, unpublished data), even though a decrease in the amount of the protease could be detected in cells treated with PMA (Figure 4; Doedens and Black, 2000).

To biochemically analyze whether TACE was involved in the cleavage of TrkA, we used a fibroblastic cell line ($TACE^{\Delta Zn/\Delta Zn}$ cells) derived from mice homozygous for a form of TACE in which the metal binding pocket of the protease had been deleted (Reddy *et al.*, 2000). This deletion leaves a continuous in-frame sequence. As a consequence, $TACE^{\Delta Zn/\Delta Zn}$ cells expressed a TACE form with an M_r below that of TACE from wild-type animals (Figure 3C). The effect of agents that in CHO^{TrkA} and 293^{TrkA} cells stimulated holoreceptor cleavage by independent MAPK routes was analyzed in several distinct clones of $TACE^{\Delta Zn/\Delta Zn}$ cells transfected with TrkA. Treatment with PMA did not induce cleavage of the holoreceptor in $TACE^{\Delta Zn/\Delta Zn}$-TrkA cells (Figure 3D). In these cells, high salt or sorbitol stimulated TrkA cleavage, indicating that cleavage mechanisms other than those induced by PKC were preserved in $TACE^{\Delta Zn/\Delta Zn}$-TrkA cells. PMA stimulated Erk1/2 phosphorylation in $TACE^{\Delta Zn/\Delta Zn}$-TrkA cells (Díaz-Rodríguez, Montero, Esparís-Ogando, Yuste, and Pandiella, unpublished data), demonstrating that the failure of the phorbol ester to induce TrkA cleavage was not due to inefficient activation of the Erk1/2 pathway.

To reconstitute TrkA cleavage in $TACE^{\Delta Zn/\Delta Zn}$-TrkA cells, we infected these cells with retrovirus that included a bicistronic vector coding for TACE and GFP (pLZR-TACE-IRES-GFP). Immunofluorescence experiments indicated that >99% of the cells that stained strongly for TACE also exhibited a strong GFP signal (Díaz-Rodríguez, Montero, Esparís-Ogando, Yuste, and Pandiella, unpublished data). Retroviral infection forced the expression of wild-type TACE to levels several times higher than those for endogenous TACE-ΔZn^{2+} (Figure 3E, bottom). In cells expressing wild-type TACE, treatment with PMA induced p41/40 generation, in contrast to cells infected with the retrovirus containing the empty vector pLZR-IRES-GFP (Figure 3E, top). That TACE could reconstitute TrkA cleavage in $TACE^{\Delta Zn/\Delta Zn}$-TrkA cells was also supported by immunofluorescence experiments (Figure 3F). For these experiments, we used the same $TACE^{\Delta Zn/\Delta Zn}$-TrkA clone that was used for the biochemical experiments. Immunofluorescence staining with the anti-TrkA antibodies showed that, together with TrkA-expressing cells, this clone also contained a cell population that had lost TrkA expression (Figure 3F). Cells were infected with the retrovirus containing the pLZR-TACE-IRES-GFP vector, treated (Figure 3F, bottom) or not (Figure 3F, top) with PMA. Then cells were analyzed for TrkA content by staining with the anti-ectodomain and anti-endodomain antibodies. As previously reported (Cabrera *et al.*, 1996; Diaz-Rodriguez *et al.*, 1999), TrkA ectodomain cleavage can be followed by loss of anti-ectodomain fluorescence at the cell periphery with preservation of peripheral staining with the anti-endodomain antibody. In cells expressing very low levels of TACE (Figure 3F, top and bottom, arrow) TrkA at the cell periphery could easily be detected by the anti-TrkA ectodomain antibody. This was observed in both untreated (top) and PMA-treated (bottom) samples. In contrast, in cells expressing TrkA and high GFP levels (Figure 3F, bottom, asterisks), PMA induced a substantial decrease in TrkA ectodomain staining, while still preserving peripheral staining by the anti-TrkA endodomain antibody. Collectively, these results indicate that TACE acts as a protease that cleaves TrkA in response to PMA.

Erk Associates with TACE and Phosphorylates Its Intracellular Domain

MAPKs are proline-directed kinases that phosphorylate target proteins at serine or threonine residues within a minimum consensus sequence of Thr/Ser-Pro (Schaeffer and Weber, 1999; Widmann *et al.*, 1999). In addition, a Pro residue at the −2 position facilitates the preference of MAPKs for their substrates (Widmann *et al.*, 1999). Inspection of the TACE intracellular domain showed the presence of a Pro-Gln-Thr^{735}-Pro motif that fits with a potential MAPK phosphorylation site, raising the possibility that TACE could be a direct MAPK substrate (Figure 4A). In vitro kinase assays using recombinant Erk (GST-Erk) or Erk immunoprecipitated from cells stimulated with phorbol esters showed that Erk could induce phosphorylation of a GST-intracellular domain of TACE fusion protein (Figure 4A). The efficiency of phosphorylation of TACE was lower than that of a classical Erk substrate such as Elk (Figure 4A). Substitution of threonine 735 for alanine in the intracellular domain of TACE (GST-TACE-$T^{735}A$) strongly reduced the ability of anti-Erk immunoprecipitates to cause in vitro phosphorylation of the mutated GST-TACE fusion protein (Figure 4B). Phosphoamino acid analysis of GST-TACE and GST-TACE-$T^{735}A$ supported the idea that the major site phosphorylated by Erk was T^{735} (Figure 4C). These analyses also demonstrated that PMA stimulated a serine kinase that coprecipitated with Erk and was able to stimulate serine phosphorylation of GST-TACE and GST-TACE-$T^{735}A$. This serine kinase phosphorylated the part of the fusion protein corre-

Figure 5 (cont). at T^{735}. 293^{TrkA} cells were infected with retrovirus containing pLZR-IRES-GFP or pLZR-HA-$Erk2^{K52R}$-IRES-GFP and treated with PMA where indicated. Cell lysates were lysed in 1 ml of lysis buffer and 20 μl were analyzed for HA-$Erk2^{K52R}$ (top) or total Erk2 (endogenous+ HA-$Erk2^{K52R}$, second panel from top) by Western blotting. In parallel, blots were also probed with anti-pErk (third panel from top). A 200-μl aliquot was immunoprecipitated with anti-Erk2 antibodies, and the immunoprecipitates were used for in vitro kinase reactions (fourth panel from top). Another 500-μl aliquot was immunoprecipitated with the anti-TACE C terminus antibody, and the blot was probed with anti-pTP (fifth panel from top). The amount of TACE in the samples was analyzed by Western blotting with anti-TACE (bottom). (G) Phosphorylation of TACE at T^{735} upon receptor tyrosine kinase activation. 293^{TrkA} cells were incubated with EGF (10 nM) or NGF (50 ng/ml) for 20 min and then lysed and immunoprecipitated with anti-TACE. Blots were probed with anti-pTP (top) or anti-TACE (bottom) antibodies. In parallel, 20-μl aliquots of the samples were run in a 10% gel and the blot was probed with anti-pErk antibodies (middle). (H) Expression of TACE-$T^{735}A$ inhibits NGF-induced TACE phosphorylation at T^{735}. 293^{TrkA} cells were infected with retrovirus containing pLZR-TACE-IRES-GFP or pLZR-TACE-$T^{735}A$-IRES-GFP. Cells were stimulated with NGF (50 ng/ml) for 20 min and lysed, and equal amounts of protein were immunoprecipitated with anti-TACE. Blots were probed with anti-pTP (top), stripped and reprobed with anti-TACE (bottom).

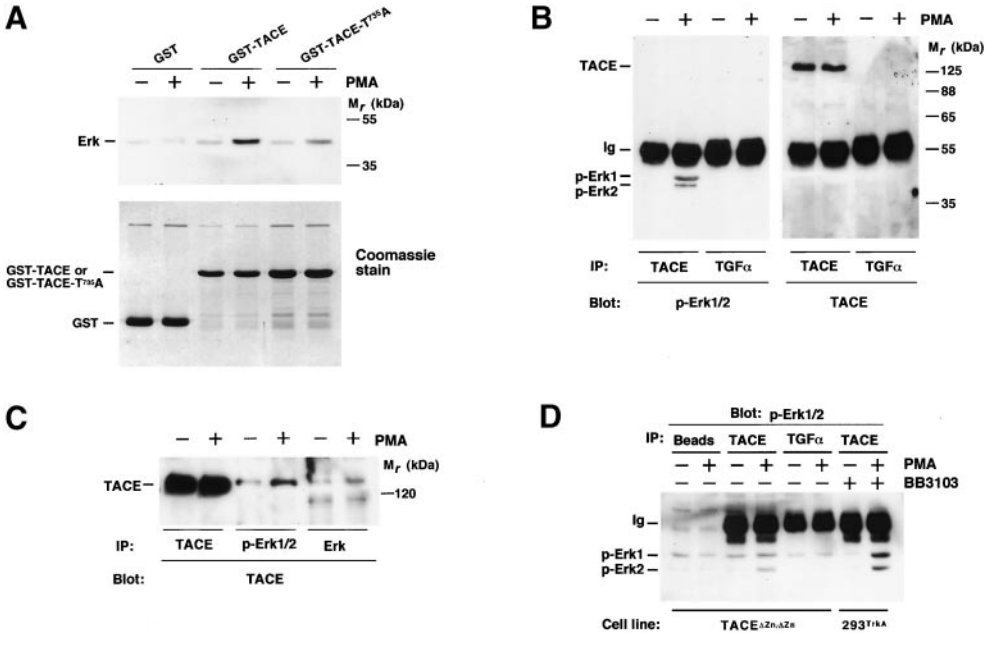

Figure 6. Association of TACE and Erk. (A) In vitro association of TACE and Erk. GST, GST-TACE, or GST-TACE-T^{735}A coupled to GSH beads was incubated with extracts from control or PMA-treated 293 cells. After incubation at 4°C, the beads were washed with PBS, and Erk associated with the beads was detected by Western blotting with the anti-Erk antibody (top). Bottom, a Coomassie stain of the GST, GST-TACE, or GST-TACE-T^{735}A loaded. (B) 293^{TrkA} cells were treated with PMA or vehicle, and lysates were immunoprecipitated with anti-TACE or anti-TGFα antibodies. Western blots were then probed with anti-Erk (left) or anti-TACE (right) antibodies. (C) 293^{TrkA} cells were treated with PMA or vehicle, and lysates were immunoprecipitated with anti-TACE, anti-p-Erk1/2, or anti-Erk antibodies, followed by Western blotting with anti-TACE antibodies. (D) Active TACE is not required for association with Erk. Extracts from control and PMA-treated TACE$^{\Delta Zn/\Delta Zn}$ cells were lysed and then protein-A-Sepharose beads were added alone (Beads) or together with the indicated antibodies (anti-TACE or anti-TGFα). In parallel, extracts from 293^{TrkA} cells pretreated with BB3103 (20 μM) were also immunoprecipitated with anti-TACE antibodies. Precipitates were washed and analyzed for Erk presence by Western blotting with anti-p-Erk antibodies.

sponding to TACE, because GST alone failed to be phosphorylated by the anti-Erk immunoprecipitates or GST-Erk (Figure 4A).

Immunoprecipitation of TACE from 293 cells labeled with ^{32}P indicated that the metalloprotease was phosphorylated under resting conditions (Figure 4D). Treatment with PMA increased the phosphorylation of TACE (Figure 4D) and caused its down-regulation (Figure 5B; see also Doedens and Black, 2000). The resting and PMA-induced increases in TACE phosphorylation were inhibited by preincubation with PD98059 (Figure 4D, bottom), suggesting that the Erk pathway participates in the control of the phosphorylation of TACE in vivo. To analyze whether T^{735} was phosphorylated in vivo, we took advantage of the fact that T^{735} is the unique Thr residue followed by a Pro in the intracellular domain of TACE (Black *et al.*, 1997; Moss *et al.*, 1997) and used an antibody that allows detection of phospho-threonine-proline (pTP) epitopes. In vitro kinase experiments indicated that this antibody reacted with GST-Elk and GST-TACE, but only when ATP was present in the incubation buffer, indicating that the antibody recognized only the phosphorylated version of these fusion proteins (Figure 5A). Recognition of GST-Elk or GST-TACE was, however, prevented when the anti-pTP antibody was preincubated with an excess of phosphothreonine (Figure 5A). In addition, the antibody failed to react with the GST-TACE-T^{735}A mutant (Figure 5B) or with GST (Díaz-Rodríguez, Montero, Esparís-Ogando, Yuste, and Pandiella, unpublished data). Western blotting of anti-TACE immunoprecipitates from 293 cells with the anti-pTP antibody indicated that TACE was phosphorylated at T^{735} under resting conditions, and PMA treatment increased phosphorylation at this site (Figure 5, C and D). Preincubation of PMA-treated extracts with an excess of the peptide used for the generation of anti-TACE antibodies (Figure 5C) or preincubation of the anti-pTP antibody with phosphothreonine (Díaz-Rodríguez, Montero, Esparís-Ogando, Yuste, and Pandiella, unpublished data) prevented the reaction of the anti-pTP antibody with TACE. Treatment of 293 cells with PD98059 decreased resting pT^{735}P TACE phosphorylation and strongly prevented the PMA-induced increase in the phosphorylation of TACE at this site (Figure 5D). In agreement with the in vitro data, an HA-tagged version of TACE mutated at T^{735} failed to be recognized by the anti-pTP antibody when transfected into 293 cells (Figure 5E).

The above data strongly indicated that TACE was phosphorylated by Erk1/2 at T^{735}. However, because PD98059 is an inhibitor of MEK1/2 (Dudley *et al.*, 1995), it was possible that a substrate of the latter, other than Erk1/2, or even MEK1/2, could be responsible for TACE phosphorylation at T^{735}. To test this possibility a dominant negative form of Erk2 was used. This form was created by point mutation (K$^{52}\rightarrow$R^{52}) in the ATP-binding pocket of the molecule. This mutation destroys the kinase activity of Erk2 but preserves MEK1/2-mediated dual phosphorylation at the Thr-Glu-Tyr microdomain within the Erk2 activation loop (see below). Infection of 293 cells with a retrovirus containing a vector for the expression of HA-tagged Erk2^{K52R} (HA-Erk2^{K52R}) resulted in the expression of the dominant negative form of the protein (Figure 5F, top) to levels above those of endogenous Erk2 (Figure 5F, second panel from top). Treatment with PMA caused a change in mobility of both endogenous Erk2 and infected HA-Erk2^{K52R} (Figure 5F, second panel from top) and induced their dual phosphorylation (Figure 5F, third panel from top). In vitro kinase studies using GST-Elk as a substrate indicated that expression of HA-

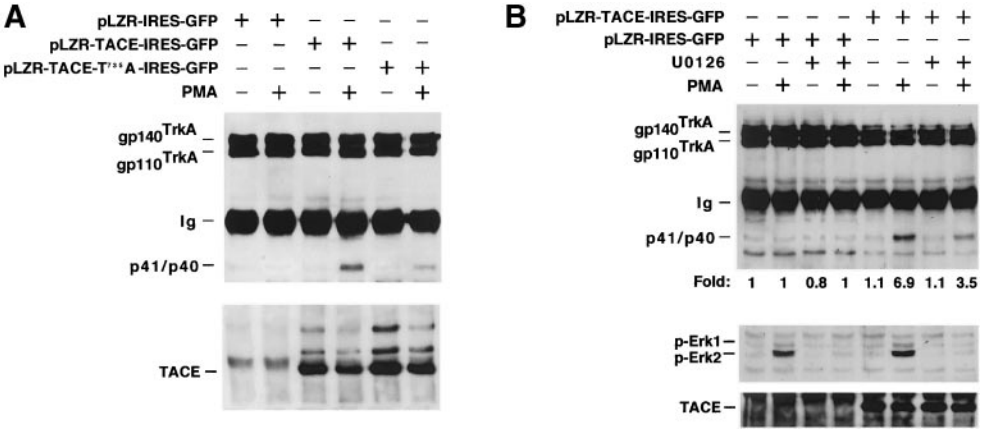

Figure 7. Effect of TACE and TACE-T^{735}A on TrkA cleavage in TACE$^{\Delta Zn/\Delta Zn}$-TrkA cells. (A) Cells were infected with pLZR-TACE-IRES-GFP, pLZR-TACE-T^{735}A-IRES-GFP, or pLZR-IRES-GFP. Cells were treated (where indicated) with PMA for 30 min. TrkA cleavage (top) and TACE content (bottom) were analyzed by Western blotting. (B) Effect of U0126 on PMA-induced TrkA cleavage in TACE$^{\Delta Zn/\Delta Zn}$-TrkA cells. Cells were infected with pLZR-TACE-IRES-GFP or with pLZR-IRES-GFP. Where indicated, U0126 (10 μM) was included in the incubation media for 30 min before PMA treatment. TrkA cleavage, p-Erk1/2, and TACE were analyzed by Western blotting as above.

Erk2^{K52R} strongly reduced Erk2 activation in response to PMA (Figure 5F, fourth panel from top). Expression of HA-Erk2^{K52R} was also able to substantially decrease resting and PMA-induced TACE phosphorylation at T^{735} (Figure 5F, second panel from bottom).

In addition to PMA, activation of receptor tyrosine kinases, such as the EGF receptor (EGFR; Fan and Derynck, [1999] or TrkA, Cabrera *et al.* [1996]; Díaz-Rodríguez, Montero, Esparís-Ogando, Yuste, and Pandiella, unpublished data), has been reported to trigger ectodomain shedding. To investigate whether receptor tyrosine kinase activation could also induce phosphorylation of TACE at T^{735}, 293^{TrkA} cells were treated with EGF or nerve growth factor (NGF). In these cells, EGF (acting through the endogenous EGFR) or NGF (acting through the transfected TrkA receptor) caused Erk1/2 activation (Figure 5G, middle) and induced TACE phosphorylation at T^{735} (Figure 5G, top). The effect of NGF on TACE phosphorylation at T^{735} was consistently more pronounced than that caused by EGF (Figure 5G; Díaz-Rodríguez, Montero, Esparís-Ogando, Yuste, and Pandiella, unpublished data), probably because of the higher complement of TrkA receptors of 293^{TrkA} cells compared with the amount of endogenous EGFR. Retrovirus-mediated expression of TACE-T^{735}A in 293^{TrkA} cells substantially reduced the ability of NGF to induce TACE phosphorylation at T^{735} (Figure 5H).

Because Erk was able to phosphorylate TACE, we investigated whether these molecules interacted. As shown in Figure 6A, the treatment of cells with PMA favored interaction of Erk with GST-TACE. Erk also interacted with GST-TACE-T^{735}A, although less efficiently than with GST-TACE. These results indicate that Erk and TACE interact in vitro and that T^{735} is important, but not critical, for the docking of Erk to the intracellular domain of TACE. To analyze whether Erk and TACE interacted in vivo, 293^{TrkA} cells were incubated with PMA and then lysates were immunoprecipitated with anti-TACE or anti-proTGFα (used as a control) antibodies. Immunoprecipitates were analyzed by SDS-PAGE followed by Western blotting with anti-p-Erk (Figure 6B, left) or anti-TACE (Figure 6B, right) antibodies. p-Erk1/2 coprecipitated with the anti-TACE immunoprecipitates but not with the anti-proTGFα immunoprecipitates. The reverse use of these antibodies confirmed that Erk and TACE coprecipitated (Figure 6C) and their interaction was favored by the activation of Erk by PMA. TACE and Erk associated in TACE$^{\Delta Zn/\Delta Zn}$ cells, as well as in 293^{TrkA} cells treated with BB3103, indicating that TACE was not required in its active form for its association to Erk (Figure 6D).

Phosphorylation of TACE at T^{735} Facilitates PMA-induced Accumulation of Truncated Fragments of TrkA

To investigate the functional importance of TACE phosphorylation at T^{735}, TACE$^{\Delta Zn/\Delta Zn}$-TrkA cells were infected with TACE or TACE-T^{735}A and TrkA cleavage in response to PMA analyzed by Western blotting. As shown above (Figure 3E), wild-type TACE rescued PMA-induced TrkA cleavage (Figure 7A). TACE-T^{735}A also rescued PMA-induced TrkA cleavage, although to a lesser extent than wild-type TACE (Figure 7A). Considering the rescue obtained with wild-type TACE as 100%, densitometric quantitation of different experiments (n = 7) indicated that TACE-T^{735}A rescued cleavage of TrkA by 59% ± 12, i.e., 41% less than wild-type TACE. The extent of this inhibition was analogous to the effect that U0126 had in these cells on PMA-induced TrkA cleavage (Figure 7B). These results demonstrate that the phosphorylation of TACE at T^{735} facilitates the accumulation of truncated fragments of TrkA, especially in cells treated with PMA. In addition, these experiments indicate that other Erk-independent routes regulate TACE activity by PMA.

DISCUSSION

In this work we report that the Erk and p38 MAPK routes act as mediators in the cleavage of TrkA induced by PKC activation or stress, respectively. We also provide evidence indicating that PMA-induced TrkA cleavage involves Erk activation. Activation of Erk facilitates its interaction with the membrane secretase TACE. We identify TACE as a novel Erk substrate and show that phosphorylation of TACE at T^{735} is important for the regulation of TACE activity by Erk.

Previous work on TrkA has indicated that PKC enzymes regulate holoreceptor cleavage (Cabrera *et al.*, 1996). The use

of inhibitors of the Erk1/2 pathway demonstrated that Erk acted as an intermediate in the action of PKC on TrkA cleavage. However, because the block was only partial, these data indicate that PKC regulates TrkA shedding by Erk-dependent and Erk-independent routes, a conclusion also supported by the reconstitution data obtained with the TACE- $T^{735}A$ mutant. Cleavage of TrkA was also induced by UV, which did not significantly induce Erk1/2 activation but stimulated p38 and JNK, indicating that other MAPK routes may regulate TrkA cleavage. This was supported by the use of the p38 pathway inhibitor SB203580. This drug, which did not affect PMA-induced TrkA cleavage, had, however, a profound effect on UV-induced receptor processing, indicating that the p38 kinase pathway mediated the action of UV on TrkA cleavage. In addition to TrkA, the p38 route has also been implicated in the shedding of L-selectin (Rizoli *et al.*, 1999) and proTGFα (Fan and Derynck, 1999), supporting the idea that this MAPK route may play a generic role in the control of membrane protein ectodomain cleavage. In a more ample context, the data obtained with different activators of cleavage together with inhibitory drugs of distinct MAPK routes suggest that MAPKs regulate the cleavage of membrane proteins by independent routes.

Our data answered the question of whether a single secretase could be activated by all the stimuli that induce cleavage. In cells expressing an inactive form of TACE, TrkA cleavage was defective, suggesting a role of this protease in PMA-induced TrkA shedding. That this secretase had a role in TrkA processing was further supported by the rescue of TrkA cleavage in response to PKC activation in $TACE^{\Delta Zn/\Delta Zn}$ cells in which wild-type TACE was reintroduced. However, secretases other than TACE may also cleave membrane proteins, because osmotic stress was able to stimulate TrkA cleavage in these cells. These findings, besides suggesting a role of TACE as a mediator of PMA-induced TrkA cleavage, also indicate that the osmotic stress-activated protease is insensitive to PKC/Erk-induced activation but is a target of the p38 route. The nature of the p38-activated (and PKC/Erk-insensitive) secretase is presently unknown. Thus, an important conclusion that emanates from these data is that a single secretase or group of secretases may be activated by some (but not all) of the intracellular routes that trigger membrane protein ectodomain cleavage.

Insights into the mechanism by which MAPKs regulate membrane protein ectodomain cleavage have been obtained by the study of TACE as a target of MAPKs. In vitro analysis indicated that the protease was phosphorylated not only by recombinant Erk but also by endogenous Erk. Substitution of the potential MAPK phosphorylation site (Thr^{735} for Ala) in TACE profoundly inhibited the ability of recombinant TACE to be phosphorylated by activated Erk, suggesting that this residue could act as a target for MAPK phosphorylation. This was further supported by the in vivo phosphorylation studies, which showed resting, growth factor, and PMA-stimulated TACE phosphorylation at T^{735}. Besides acting as a phosphorylation site, T^{735} was found to contribute to the interaction of TACE and Erk. In fact, association of Erk with TACE was favored by the presence of T^{735}, indicating that T^{735} participates in the docking of Erk to the TACE intracellular domain. This latter role, together with the fact that T^{735} phosphorylation is modestly stimulated by PMA, indicates that phosphorylation of TACE at T^{735} may not be the only signal that controls its activity, and docking of Erk may also be important, perhaps allowing Erk to target other TACE-bound molecules.

A functional role of TACE phosphorylation at T^{735} was indicated by the effect of TACE and TACE-$T^{735}A$ on the amount of truncated fragments of TrkA. In $TACE^{\Delta Zn/\Delta Zn}$ cells, TACE and TACE-$T^{735}A$ caused accumulation of the truncated fragments of TrkA, especially when cells were treated with PMA. However, the mutated form of TACE was less efficient than the wild type. This effect has also been found when analyzing the effect of TACE and TACE-$T^{735}A$ on the generation of truncated fragments of the membrane-anchored growth factor proNeuregulinα2c (J.C. Montero, L. Yuste, E. Díaz-Rodríguez, A. Esparís-Ogando, and A. Pandiella, unpublished data). How can TACE phosphorylation at T^{735} regulate the amount of the cell-bound truncated fragments? A mechanism could include the potential regulation of the catalytic activity of TACE by phosphorylation at T^{735}. However, PMA-induced shedding of TNF-α has been reported to occur independently of the cytosolic tail of TACE (Reddy *et al.*, 2000). On the other hand, TACE phosphorylation at T^{735} could regulate the amount of the cell-bound truncated fragments by mechanisms not related to the control of TACE activity. Thus, TACE could favor the stabilization of the truncated fragments by decreasing their turnover and the TACE-$T^{735}A$ mutant could be less effective. However, we have failed to detect any significant difference in the resting accumulation of truncated fragments of TrkA between $TACE^{\Delta Zn/\Delta Zn}$-TrkA cells infected with TACE or TACE-$T^{735}A$. Another possibility could be the participation of T^{735} phosphorylation in the maturation of TACE with generation of the processed, active form of the enzyme. In this respect, it is interesting that the phosphorylated form of TACE detected in 293 cells corresponds to unprocessed TACE. Finally, another mechanism that could explain why TACE causes accumulation of TrkA and proNRGα2c fragments better than TACE-$T^{735}A$ could be related to a potential sorting defect of the mutated TACE. This latter possibility seems unlikely because cell surface immunoprecipitation of HA-tagged forms of TACE and TACE-$T^{735}A$ reveal identical exposure of wild type and the mutant protein at the cell surface (L. Yuste and A. Pandiella, unpublished observations). A detailed study of TACE phosphorylation, maturation, sorting/trafficking, and shedding activity will be required to address the above possibilities.

In summary, our data indicate that multiple MAPK routes independently regulate membrane protein ectodomain cleavage and show that secretases are able to discriminate between the ample spectrum of stimuli that induce cleavage. In addition, we identified TACE as a novel Erk substrate and described a potential mechanism of activation of TACE by Erk. The future identification of other functional secretases and their cellular targets will allow us to evaluate to which extent direct phosphorylation by MAPKs regulates the activity of other membrane secretases.

ACKNOWLEDGMENTS

We particularly thank Drs. Jacques Peschon, and Roy. A. Black, from Immunex, for providing us with the $TACE^{\Delta Zn/\Delta Zn}$ cells, the M220 antibody, and the mouse TACE cDNA. The supply of BB3103 by British Biotech is also acknowledged. We thank Dr. X. Bustelo for reading the manuscript and continuous encouragement. This work

was funded by the European Community, the Fundación Ramón Areces, and the Spanish Ministry of Education and Culture. E.D-R. was supported by a fellowship from the Centro de Investigación del Cáncer. A.E-O. was supported by a postdoctoral contract from the Spanish Ministry of Education and Culture, and L.Y was supported by a predoctoral fellowship from the same Ministry.

REFERENCES

Black, R.A., Rauch, C.T., Kozlosky, C.J., Peschon, J.J., Slack, J.L., Wolfson, M.F., Castner, B.J., Stocking, K.L., Reddy, P., Srinivasan, S., Nelson, N., Boiani, N., Schooley, K.A., Gerhart, M., Davis, R., Fitzner, J.N., Johnson, R.S., Paxton, R.J., Marc, C.J., and Cerretti, D.P. (1997). A metalloproteinase disintegrin that releases tumor-necrosis factor-alpha from cells. Nature *385,* 729–733.

Black, R.A., and White, J.M. (1998). ADAMs: focus on the protease domain. Curr. Opin. Cell Biol. *10*, 654–659.

Blobel, C.P. (1997). Metalloprotease-disintegrins: links to cell adhesion and cleavage of TNF alpha and Notch. Cell *90*, 589–592.

Buxbaum, J.D., Liu, K.N., Luo, Y., Slack, J.L., Stocking, K.L., Peschon, J.J., Johnson, R.S., Castner, B.J., Cerretti, D.P., and Black, R.A. (1998). Evidence that tumor necrosis factor alpha converting enzyme is involved in regulated alpha-secretase cleavage of the Alzheimer amyloid protein precursor. J. Biol. Chem. *273*, 27765–27777.

Cabrera, N., Díaz-Rodríguez, E., Becker, E., Zanca, D.M., and Pandiella, A. (1996). TrkA receptor ectodomain cleavage generates a tyrosine-phosphorylated cell-associated fragment. J. Cell Biol. *132*, 427–436.

Cohen, P. (1997). The search for physiological substrates of MAP and SAP kinases in mammalian cells. Trends Cell Biol. *7,* 353–361.

Cooper, J.A., Sefton, B.M., and Hunter, T. (1983). Detection and quantification of phosphotyrosine in proteins. Methods Enzymol. *99,* 387–402.

Diaz-Rodriguez, E., Cabrera, N., Esparís-Ogando, A., Montero, J.C., and Pandiella, A. (1999). Cleavage of the TrkA neurotrophin receptor by multiple metalloproteases generates signaling-competent truncated forms. Eur. J. Neurosci. *11*, 1421–1430.

Doedens, J.R., and Black, R.A. (2000). Stimulation-induced down-regulation of tumor necrosis factor-alpha converting enzyme. J. Biol. Chem. *275*, 14598–14607.

Downing, J.R., Roussel, M.F., and Sherr, C.J. (1989). Ligand and protein kinase C downmodulate the colony-stimulating factor 1 receptor by independent mechanisms. Mol. Cell. Biol. *9*, 2890–2896.

Dudley, D.T., Pang, L., Decker, S.J., Bridges, A.J., and Saltiel, A.R. (1995). A synthetic inhibitor of the mitogen-activated protein kinase cascade. Proc. Natl. Acad. Sci. USA *92*, 7686–7689.

Ehlers, M.R.W., and Riordan, J.F. (1991). Membrane proteins with soluble counterparts: role of proteolysis in the release of transmembrane proteins. Biochemistry *30,* 10065–10074.

Fan, H., and Derynck, R. (1999). Ectodomain shedding of TGF-alpha and other transmembrane proteins is induced by receptor tyrosine kinase activation and MAP kinase signaling cascades. EMBO J. *18,* 6962–6972.

Favata, M.F., Horiuchi, K.Y., Manos, E.J., Daulerio, A.J., Stradley, D.A., Feeser, W.S., Van Dyk, D.E., Pitts, W.J., Earl, R.A., Hobbs, F., Copeland, R.A., Magolda, R.L., Scherle, P.A., and Trzaskos, J.M. (1998). Identification of a novel inhibitor of mitogen-activated protein kinase kinase. J. Biol. Chem. *273*, 18623–18632.

Garrington, T.P., and Johnson, G.L. (1999). Organization and regulation of mitogen-activated protein kinase signaling pathways. Curr. Opin. Cell Biol. *11*, 211–218.

Gearing, A.J.H., Beckett, P., Christodoulou, M., Churchill, M., Clements, J., Davidson, A.H., Drummond, A.H., Galloway, W.A., Gilbert, R., Gordon, J.L., *et al.* (1994). Processing of tumor necrosis factor-alpha precursor by metalloproteinases. Nature *370,* 555–557.

Gechtman, Z., Alonso, J.L., Raab, G., Ingber, D.E., and Klagsbrun, M. (1999). The shedding of membrane-anchored heparin-binding epidermal-like growth factor is regulated by the Raf/mitogen-activated protein kinase cascade and by cell adhesion and spreading. J. Biol. Chem. *274*, 28828–28835.

Guan, K.L., and Dixon, J.E. (1991). Eukaryotic proteins expressed in *Escherichia coli*: an improved thrombin cleavage and purification procedure of fusion proteins with glutathione *S*-transferase. Anal. Biochem. *192*, 262–267.

Hooper, N.M., Karran, E.H., and Turner, A.J. (1997). Membrane protein secretases. Biochem. J. *321*, 265–279.

Ip, Y.T., and Davis, R.J. (1998). Signal transduction by the c-Jun N-terminal kinase (JNK): from inflammation to development. Curr. Opin. Cell Biol. *10*, 205–219.

Izumi, Y., Hirata, M., Hasuwa, H., Iwamoto, R., Umata, T., Miyado, K., Tamai, Y., Kurisaki, T., Sehara-Fujisawa, A., Ohno, S., and Mekada, E. (1998). A metalloprotease-disintegrin, MDC9/meltrin-gamma/ADAM9 and PKCdelta are involved in TPA-induced ectodomain shedding of membrane-anchored heparin-binding EGF-like growth factor. EMBO J. *17,* 7260–7272.

Kishimoto, T.E., Jutila, M.A., Berg, E.L., and Butcher, E.C. (1989). Neutrophil Mac-1 and MEL-14 adhesion proteins inversely regulated by chemotactic factors. Science *245,* 1238–1241.

Massagué, J., and Pandiella, A. (1993). Membrane-anchored growth factors. Annu. Rev. Biochem. *62*, 515–541.

McDermott, M.F., *et al*. (1999). Germline mutations in the extracellular domains of the 55 kDa TNF receptor, TNFR1, define a family of dominantly inherited autoinflammatory syndromes. Cell *97,* 133–144.

McGeehan, G.M., *et al.* (1994). Regulation of tumor necrosis factor-α by a metalloproteinase inhibitor. Nature *370,* 558–561.

Mohler, K.M., Sleath, P.R., Fitzner, J.N., Cerretti, D.P., Alderson, M., Kerwar, S.S., Torrance, D.S., Otten-Evans, C., Greenstreet, T., Weerawarna, K., *et al.* (1994). Protection against a lethal dose of endotoxin by an inhibitor of tumor necrosis factor processing. Nature *370,* 218–220.

Moss, M.L., et al. (1997). Cloning of a disintegrin metalloproteinase that processes precursor tumor necrosis factor-α. Nature *385,* 733–736.

Nebreda, A.R., and Porras, A. (2000). p38 MAP kinases: beyond the stress response. Trends Biochem. Sci. *25*, 257–260.

Peschon, J.J., et al. (1998). An essential role for ectodomain shedding in mammalian development. Science *282,* 1281–1284.

Porteu, F., and Nathan, C. (1990). Shedding of tumor necrosis factor receptors by activated human neutrophils. J. Exp. Med. *172*, 599–607.

Prat, M., Crepaldi, T., Gandino, L., Giordano, S., Longati, P., and Comoglio, P. (1991). C-terminal truncated forms of Met, the hepatocyte growth factor receptor. Mol. Cell. Biol. *11*, 5954–5962.

Reddy, P., Slack, J.L., Davis, R., Cerretti, D.P., Kozlosky, C.J., Blanton, R.A., Shows, D., Peschon, J., and Black, R.A. (2000). Functional analysis of the domain structure of tumor necrosis factor-α converting enzyme. J. Biol. Chem. *275*, 14608–14616.

Rizoli, S.B., Rotstein, O.D., and Kapus, A. (1999). Cell volume-dependent regulation of L-selectin shedding in neutrophils: a role for p38 mitogen-activated protein kinase. J. Biol. Chem. *274*, 22072–22080.

Robinson, M.J., and Cobb, M.H. (1997). Mitogen-activated protein kinase pathways. Curr. Opin. Cell Biol. *9*, 180–186.

Sadhukhan, R., Santhamma, K.R., Reddy, P., Peschon, J.J., Black, R.A., and Sen, I. (1999). Unaltered cleavage and secretion of angiotensin-converting enzyme in tumor necrosis factor-alpha-converting enzyme-deficient mice. J. Biol. Chem. *274*, 10511–10516.

Schaeffer, H.J., and Weber, M.J. (1999). Mitogen-activated protein kinases: specific messages from ubiquitous messengers. Mol. Cell. Biol. *19*, 2435–2444.

Selkoe, D.J. (1994). Cell biology of the amyloid β-protein precursor and the mechanism of Alzheimer's disease. Annu. Rev. Cell Biol. *10*, 373–403.

Tanoue, T., Adachi, M., Moriguchi, T., and Nishida, E. (2000). A conserved docking motif in MAP kinases common to substrates, activators and regulators. Nat. Cell Biol. *2*, 110–116.

Vecchi, M., Baulida, J., and Carpenter, G. (1996). Selective cleavage of the heregulin receptor ErbB-4 by protein kinase C activation. J. Biol. Chem. *271*, 18989–18995.

Widmann, C., Gibson, S., Jarpe, M.B., and Johnson, G.L. (1999). Mitogen-activated protein kinase: conservation of a three-kinase module from yeast to human. Physiol. Rev. *79*, 143–180.

Yee, N.S., Hsiau, C.-W., Serve, H., Vosseler, K., and Besmer, P. (1994). Mechanism of down regulation of c-*kit* receptor. J. Biol. Chem. *269*, 31991–31998.